Dynamics of cavity solitons in fiber cavities and microresonators in the normal dispersion regime

P. Parra-Rivas,[1,2] D. Gomila,[2] L. Gelens,[1,3] and E. Knobloch[4]

[1] Applied Physics Research Group, APHY, Vrije Universiteit Brussel, 1050 Brussels Belgium.
[2] Instituto de Física Interdisciplinar y Sistemas Complejos, IFISC (CSIC-UIB),Campus Universitat de les Illes Balears, E-07122 Palma de Mallorca, Spain.
[3] Dept. of Chemical and Systems Biology, Stanford University School of Medicine, Stanford CA 94305-5174, USA.
[3] Department of Physics, University of California, Berkeley, CA 94720

In this work we present a general analysis of the regions of existence and stability of dark solitons in the Lugiato-Lefever model with normal dispersion. In this regime the localized states are organized in a bifurcation structure known as collapsing snaking. After characterizing the unfolding of that structure, we determine the regions of multistability of solitons in parameter space. We show that for some sets of parameters several dynamical instabilities, responsible for the appearing of oscillations and temporal chaos, can occur. Finally we emphasize the importance of these results in understanding frequency comb generation in microresonators.

Introduction to the model

The Lugiato-Lefever (LL) model was first introduced in 1987 as a mean field model to describe a ring cavity with a transverse spatial extension and partially filled with a nonlinear medium [1]. Lately the same model was found to describe the propagation of pulses in a fiber cavity pumped by an external field [2]. Here, without lost of generality we will focus on microresonators like the one shown in Figure 1. This device is characterized by a length L a beam splitter with transmission coefficient T, and a source such as a mode-locked laser that emits a train of pulses of amplitude E_0. At the beam splitter, this pulse train is added to the electromagnetic wave circulating inside the fiber at the beam splitter. Here we consider that the amplitude of the pulses is small and they can be approximated by a continuous wave (CW) E_0. We also assume that the pulse duration is much shorter than the round-trip time t_R of the cavity given by $t_R = L/c$ (with c the speed of light in the medium). Under those conditions the evolution of the optical field $E = E(t,\tau)$ within the

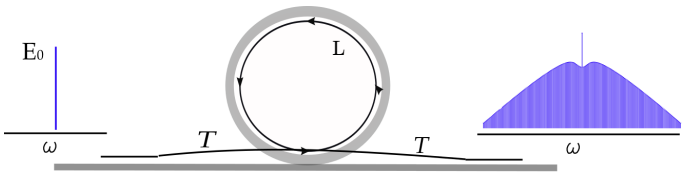

Figure 1: A synchronously pumped fiber cavity. T is the transmission coefficient of the beam splitter. L is the length of the fiber.

cavity after each round-trip is described by the following equation [2]:

$$t_R\frac{\partial E}{\partial t'} = -(\alpha + i\delta_0)E - i\frac{L\beta_2}{2}\frac{\partial^2 E}{\partial \tau'^2} + i\Gamma L|E|^2 + \sqrt{T}E_0, \tag{1}$$

where α describes the total cavity losses, β_2 is the second order dispersion coefficient ($\beta_2 > 0$ in the normal dispersion case and $\beta_2 < 0$ in the anomalous one), Γ is the nonlinear coefficient due to the Kerr effect in the resonators, and δ_0 is the cavity detuning. The slow time t describes the wave evolution after each round-trip and τ is the fast time describing the temporal structure of the nonlinear waves. In this work we will focus on the normal dispersion regime and therefore we will consider that $\beta_2 > 0$. After normalizing Eq.(1) we arrive to the dimensionless mean-field LL equation [1]:

$$\partial_t u = -(1 + i\theta)u - i\partial_\tau^2 u + iu|u|^2 + u_0 \tag{2}$$

with $t = \alpha t'/t_R$, $\tau = \tau'\sqrt{2\alpha/(L\beta_2)}$, $u(t,\tau') = E(t',\tau')\sqrt{\Gamma L/\alpha}$, $u_0 = E_0\sqrt{\Gamma L T/\alpha^3}$, and $\theta = \delta_0/\alpha$. In the following we will not consider any potential higher order dispersion effects as analyzed in Refs. [3, 4, 5, 6].
u is a complex scalar field and u_0, θ are real parameters corresponding to the normalized injection and the detuning respectively. In the following they will be the control parameters of the system. Due to the periodic nature of microresonators, in this study we will consider periodic boundary conditions and we chose the normalized length $L = 160$. The CW or homogeneous steady state (HSS) solutions u_h of Eq.(2) satisfy classic cubic equation of dispersive optical bistability, namely

$$I^3 - 2\theta I^2 + (1 + \theta^2)I = u_0^2 \tag{3}$$

where $I = |u_h|^2$. For $\theta < \sqrt{3}$, Eq.(3) is monovaluate and hence the system is monostable. For $\theta > \sqrt{3}$, Eq.(3) is trivaluate as we observe in Figs.2(a). The transition between the three different solutions happens through the saddle-nodes $\mathrm{SN}_{hom,1}$ and $\mathrm{SN}_{hom,2}$ located at

$$I_\pm = \frac{2\theta}{3} \pm \frac{1}{3}\sqrt{\theta^2 - 3}. \tag{4}$$

In the following we will denote by u_h^b the bottom branch of solutions (from $I = 0$ to I_-), the middle branch between I_- and I_+ by u_h^m and the top branch by u_h^t ($I > I_+$).

Dark solitons in the normal dispersion regime

In anomalous dispersion regime, bright solitons solutions of Eq.(2), were organized in bifurcation structure known as homoclinic snaking [7, 8, 9, 10]. On the contrary here, the most common structures are dark solitons and we found are organize in a collapsing snaking bifurcation structure [11]. In Figure 2 we show a collapsing snaking for $\theta = 4$. To build this diagram, we first applied a weakly nonlinear analysis around $\mathrm{SN}_{hom,2}$ to obtain a asymptotic approximation to the solution (only valid in the vicinity of that point). After, we apply continuation techniques that allow us to calculate the solution of Eq.(2) for parameters further from $\mathrm{SN}_{hom,2}$. Initially dark solitons that unfolds from $\mathrm{SN}_{hom,2}$ are unstable. Increasing the parameter u_0 those states reach the saddle-node SN_1 where they become stable. This solution is like the one shown in Figure 2 (i). Decreasing u_0,

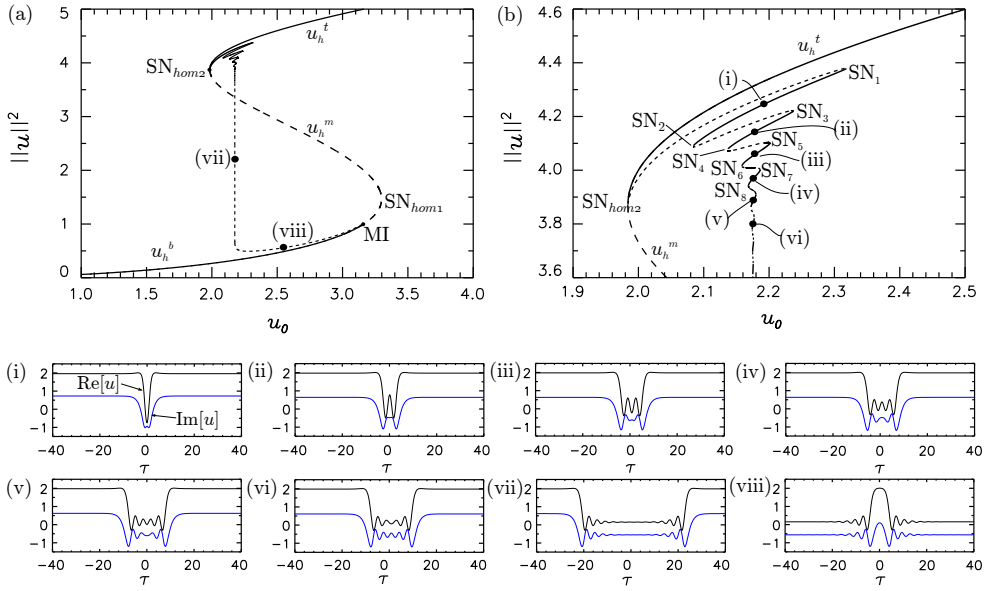

Figure 2: Panel (a) shows the bifurcation diagram for $\theta = 4$ showing the collapsing the snaking and the reconnection with the MI in the bottom HSS branch. Panel (b) shows a zoom of the collapsing snaking of the first panel. The bottom panels are labeled with (i),...,(viii) are the cavity solitons corresponding to the same labels in panels (a) and (b).

the solution branch ends in a SN_2 where it becomes unstable. Together with this change of stability spatial oscillations (SO) are added to the profile of the field as we can see in Figure 2 (ii). Moving forward and backward on u_0, this process is repeated and at every saddle-node extra SOs are added to the state. When adding new SO, the region of existence shrinks until the snaking collaps to a vertical branch that approaches the Maxwell point of the system. At that stage dark solitons correspond to a hole state like the one shown in Figure 2 (vii). This kind of hole solution can be understood as two front solutions connecting first u_h^t with u_h^b and after u_h^b with u_h^t. Decreasing the norm, the separation of those fronts increase, until due to the periodicity they reach the size of the system resulting a state like the one shown in Figure 2 (viii). This solution belongs to a branch that extends from the Maxwell point to the modulational instability (MI) occurring at $||u||^2 = 1$, from where it unfolds.

Oscillatory and chaotic dynamics

In normal dispersion case, as in the anomalous dispersion case [8, 9], oscillatory and chaotic dynamics are also found for high values of detuning. In Figure 3 we show the collapsing snaking corresponding to $\theta = 10$. In that diagram we can observe how the solution branches corresponding to one and two SO dark solitons become unstable through Hopf bifurcations (H_1, H_2) to oscillatory states. Two examples of those oscillons can be see also in panels (i) and (ii) in Figure 3. Chaotic dynamics are also found in this regime and for the interested reader we refer to Ref.[12].

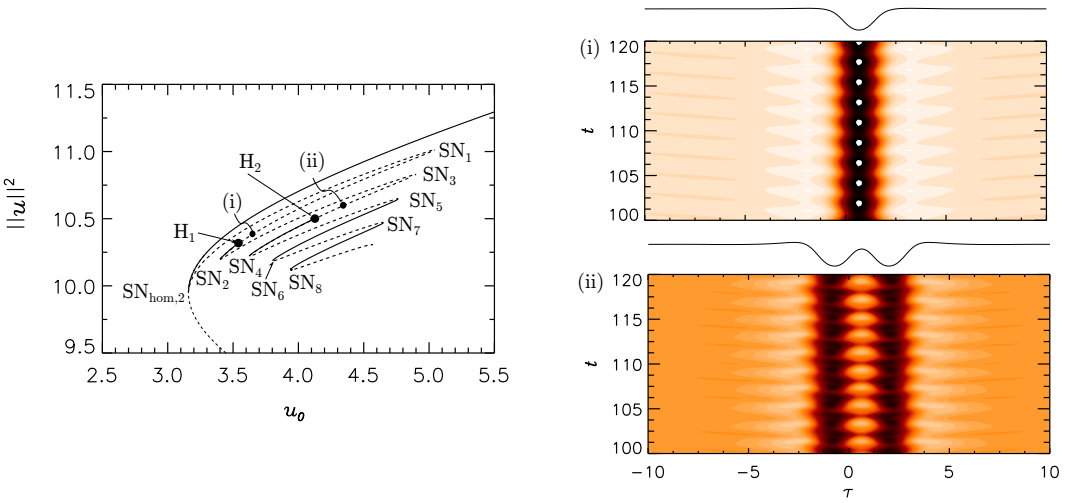

Figure 3: Bifurcation diagram for $\theta = 10$, and oscillatory states with one (i) and two (ii) SOs

Conclusions

In this work we have presented the bifurcation structure and stability of the dark solitons in the normal dispersion regime. We have also shown that for high values of θ those solitons become oscillatory unstable. Due to the the strong correspondence between Kerr temporal solitons and frequency combs (FCs), the system reported here have recently attracted a lot of interest [13]. FCs consist in a set of equidistant spectral lines that can be use to measure light frequencies an time intervals more easily and precisely than ever before [14, 15]. For further information on this work we refer to Ref.[12].

References

[1] L. A. Lugiato, and R. Lefever, Phys. Rev. Lett. **58**, 2209 (1987).

[2] M. Haelterman, S. Trillo, and S. Wabnitz, Opt. Comm. **91**, 401-407 (1992).

[3] L. Gelens, G. Van der Sande, P. Tassin, M. Tlidi, P. Kockaert, D. Gomila, I. Veretennicoff and J. Danckaert, Phys. Rev. A **75,** 063812 (2007).

[4] L. Gelens, D. Gomila, G. Van der Sande, J. Danckaert, P. Colet, and M. A. Matías, Phys. Rev. A **77,** 033841 (2008).

[5] M. Tlidi and L. Gelens, Opt. Lett. **35,** 306 (2010).

[6] P. Parra-Rivas, D. Gomila, F. Leo, S. Coen and L. Gelens, Opt. Lett. **39**, 2971-2974 (2014).

[7] D. Gomila, A. J. Scroggie, and W. J. Firth, Phys. D (Amsterdam) 227, 70 (2007).

[8] F. Leo, L. Gelens, P. Emplit, M. Haelterman, and S. Coen, Opt. Express **21**, 9180 (2013).

[9] P. Parra-Rivas, D. Gomila, M. A. Matias, S. Coen, and L. Gelens, Phys. Rev. A **89**, 043813 (2014).

[10] C. Godey, I. V. Balakireva, A. Coillet, and Y. K. Chembo Phys. Rev. A **89**, 063814

[11] J. Burke, A. Yochelis, and E. Knobloch, Phys. D (Amsterdam) *239*, 1867-1883 (2010).

[12] P. Parra-Rivas, D. Gomila, L. Gelens, and E. Knobloch (in preparation).

[13] S. Coen, H. G. Randle, T. Sylvestre, and M. Erkintalo, Opt. Lett. **38**, 37 (2013); S. Coen and M. Erkintalo, Opt. Lett. **38**, 1790 (2013); Y. K. Chembo and C. R. Menyuk, Phys. Rev. A **87**, 053852 (2013).

[14] S. Cundiff, J. Ye, and J. Hall, Sci. Am. **298**, 74 (2008)

[15] P. Del'Haye, A. Schliesser, O. Arcizet, T. Wilken, R. Holzwarth, and T. J. Kippenberg, Nature (London) **450**, 1214 (2007).